ARTICLE

A solvent-mediated conformational switch in sulfanilamide

Sergio Mato, [a] Raúl Aguado, [a] Santiago Mata, [a] José Luis Alonso [a] and Iker León,*[a]

Received 00th January 20xx,
Accepted 00th January 20xx

DOI: 10.1039/x0xx00000x

Sulfanilamide, a widely used antibacterial drug, has been brought into the gas phase using laser ablation techniques, and its structure has been characterized in the isolated conditions of a supersonic expansion using Fourier transform microwave techniques. A single conformer stabilized by an N-H•••O=S intramolecular interaction in an equatorial disposition has been unequivocally characterized. To emulate the microsolvation process, we studied its hydrated cluster. The results show that a single water molecule alters the conformational preference and forces sulfanilamide to switch from its initial eclipsed configuration to a staggered disposition. The observed hydrated cluster adopts a structure in which water forms three hydrogen bonds with sulfanilamide stabilizing the molecule.

Introduction

Sulfanilamide (SA, 4-aminobenzenesulfonamide), shown in Scheme 1, is a synthetic molecule consisting of an aniline derivatized with a sulfonamide group. It was discovered in 1908[1] and was initially employed as an antibacterial drug to reduce infection rates.[2] Moreover, SA is used as a core for developing more effective derivatives with different bioactivities. Sulfa drugs are competitive inhibitors of p-aminobenzoic acid (PABA) in the folic acid metabolism cycle in organisms.[3–6] Specifically, it competitively inhibits the enzyme dihydropteroate synthase (DHPS) by interacting with the same activity center. This enzyme typically uses para-aminobenzoic acid (PABA) to synthesize the necessary folic acid (vitamin B9), a coenzyme, to synthesize purines and pyrimidines. The inhibited reaction usually is necessary for these organisms to synthesize folic acid. Without it, bacteria cannot replicate. Furthermore, mammals do not synthesize their own folic acid, so they are unaffected by PABA inhibitors, which selectively kill bacteria.

The competitive inhibition between sulfanilamide and PABA occurs due to their structural similarity caused by the bioisosteric replacement of the -COOH group in PABA by the -SO_2NH_2 group in sulfanilamide. Therefore, determining the spatial disposition of the atoms, the main functional groups, as well as evaluating the intra- and intermolecular forces, is a key step to understanding the biological process. Considering this, determining the isolated three-dimensional structure of the molecule is mandatory as it allows the study of its main intramolecular interactions without presenting any other external interaction that would otherwise modify its intrinsic conformation preferences. This step is crucial as it can give additional and vital information to understand the binding process within the active center.

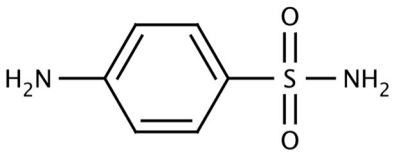

Scheme 1 Chemical structure of sulfanilamide.

Numerous studies have been carried out to determine its structure in condensed and gas phases. In condensed phases, X-ray diffraction showed four polymorphs differing in the torsion of the sulfonamide group.[7–12] FTIR, FT-Raman and NMR techniques found an eclipsed conformation.[13–15] Investigations carried out in the gas phase using matrix isolation FTIR spectroscopy in Ar and Xe matrices,[16] as well as those studies conducted using UV and IR spectroscopy,[17] found a single conformation. However, the four stable structures of the monomer show no differences in the IR spectrum, and the assignment is mainly based on the calculated energetics. A recent work conducted using gas-phase electron diffraction[18] shows that, at 184°C, conformations in an eclipsed orientation are predominant in vapor (90%), although no distinction between the orientation of the anilinic amino group is made. A recent study using rotational spectroscopy[19] shows that the eclipsed orientation is the most stable configuration, but again the preferred disposition for the orientation of the anilinic amino group is undetermined. Finally, studies conducted using UV and IR spectroscopy for the hydrated species of sulfanilamide,[17] show a single conformer, attributed to a staggered orientation, but the assignment is based on the subtle variation of a single stretching mode in less than 30 cm^{-1}. Thus, while there exists an initial assignment for the hydrated species, an accurate structural determination is still needed.

[a] *Grupo de Espectrocopía Molecular (GEM), Edificio Quifima, Laboratorios de Espectroscopia y Bioespectroscopia, Unidad Asociada CSIC, Parque Científico UVa, Universidad de Valladolid, 47011, Valladolid, Spain.*

†Electronic Supplementary Information (ESI) available: Full and selected rotational spectra, measured frequencies and residuals for the rotational transitions, relaxed PES, and bond strengths. See DOI: 10.1039/x0xx00000x

In a quest to obtain the most relevant species of sulfanilamide, we combine the benefits of chirped pulse and narrow-band Fourier-transform microwave spectroscopy with vaporization by laser ablation (LA-CP-FTMW and LA-MB-FTMW)[20–25] and apply them to sulfanilamide. Rotational spectroscopy has proven a powerful tool for unambiguously identifying chemical species in the gas phase and is acknowledged among the most robust techniques to distinguish between subtle changes in molecular geometry. Since every molecule has a unique three-dimensional structure, it possesses a characteristic set of rotational constants. Furthermore, due to the low vapor pressure and degradation upon heating of most of the biomolecules, as it is the case of sulfanilamide (m. p. 165°C), the use of laser ablation allowed an optimal transfer of the molecules into the gas phase. In the following, we present a rotational spectroscopic study of SA which shows an exciting outcome: as we will prove a single water molecule alters the conformational preference and forces sulfanilamide to switch from its initial eclipsed configuration to a staggered disposition.

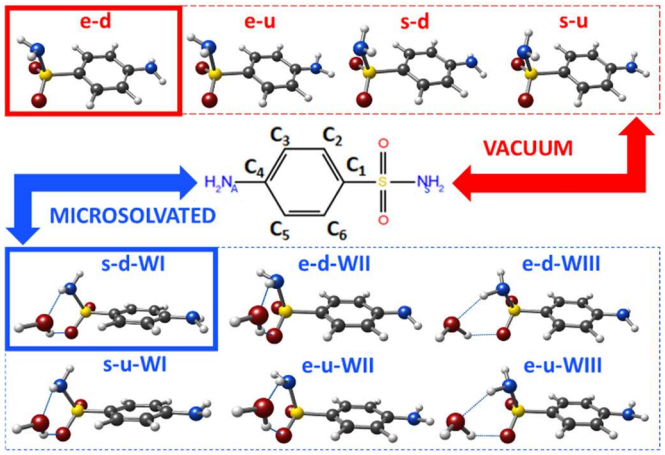

Figure 1 The four most stable structures of sulfanilamide (top) and sulfanilamide-water (bottom), calculated at B3LYP-D3(BJ)/6-311++G(d,p). The sketch of the sulfanilamide molecule is shown in the centre. Blue and red frames highlight the structures experimentally observed.

Methods

Experimental details

A commercial sample of sulfanilamide (Cymit, m.p. 165°C) was used without any further purification. A solid rod was prepared by pressing the compound's fine powder mixed with a small amount of commercial binder (Peoval). We kept it at vacuum for at least two weeks to allow it to dry, and was placed in the ablation nozzle. A picosecond Nd:YAG laser (355nm, 15 mJ per pulse, 20 ps pulse width) was used as a vaporization tool. Firstly, products of the laser ablation were supersonically expanded utilizing the flow of Helium as a carrier gas at a stagnation pressure of 5.5 bar, and characterized by chirped-pulse Fourier transform microwave spectroscopy (LA-CP-FTMW).[20–23] For the chirped pulses, a 24 GS·s^{-1} arbitrary waveform generator was used to create 4 µs length pulses in the 3–7 GHz range. These pulses were doubled (6-14 GHz) using an active multiplier, and then amplified using a 300W TWT amplifier to create a high-energy excitation pulse that polarizes the molecules in the 6-14 GHz frequency range. Up to 128000 individual free induction decays (4 FIDs on each valve cycle at a 2 Hz repetition rate) were averaged in the time domain, and then Fourier transformed to obtain the broadband frequency domain spectrum. For the hydrated cluster, no water was added and small amounts of water vapor present in the carrier gas were used.

In order to resolve the hyperfine structure, a molecular beam Fourier transform microwave spectrometer (LA-MB-FTMW) dedicated to maximize its performance in the 2-8 GHz frequency range was used.[24,25] This spectrometer provides the high-resolution necessary to analyze the hyperfine structure due to the presence of two ^{14}N nuclei in the molecule. All the transitions appeared as Doppler doublets due to the parallel configuration of the molecular beam and the microwave radiation. The resonance frequency was determined as the arithmetic means of the two Doppler components. In this setup, a picosecond Nd:YAG laser (355nm, 15 mJ per pulse, 20 ps pulse width) was used as a vaporization tool, and a flow of He/Ne of 20:80 was employed as a carrier gas at a stagnation pressure of 10 bar.

Theoretical Modelling

A conformational search of sulfanilamide and its water cluster was carried out to facilitate the identification of the different conformers present during adiabatic expansion. MMFFs forcefield and two search algorithms: the "Large scales Low Mode" (which uses frequency modes to create new structures) and a Monte Carlo-based search, as implemented in Macromodel[26] employed using a 30 kJ/mol energy cut off. A total of four different structures were obtained for the monomer, while 20 structures were found for the sulfanilamide-water cluster. The resulting geometries were then optimized by MP2[27] and B3LYP-D3 (BJ)[28–30] methods using the Pople's 6-311 ++ G (d,p) basis set.[31] For the DFT method, Grimme's dispersion correction (D3) with Becke-Johnson damping (BJ)[32] were included. This procedure resulted in a reduction from 20 to 16 conformers for the sulfanilamide-water, while the monomer showed 4 structures.

Results and Discussion

In the first step, we conducted a conformational search of sulfanilamide as explained in the previous section. This procedure allowed us to filter the most stable species relevant to our experiment, i.e., with relative energies lower than 500 cm^{-1}. For the monomer, a total of four stable species were obtained. The relevant structures are shown in Figure 1. Additionally, the values of the rotational constants, nuclear quadrupole coupling constants and the dipole moment components that will facilitate the conformational assignment are collected in Table 1. The two most stable conformers have an eclipsed configuration and they differ in the orientation of the anilinic amine group. Among them, B3LYP method predicts

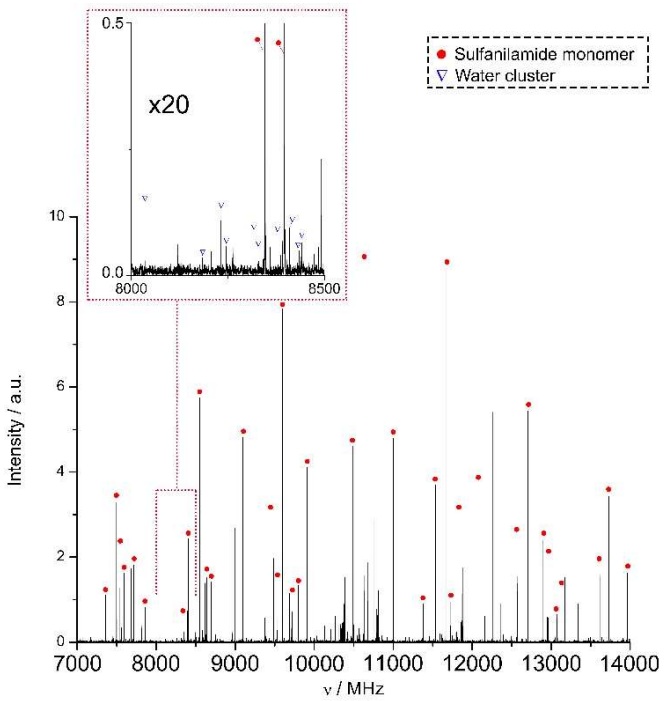

Figure 2 LA-CP-FTMW rotational spectrum of sulfanilamide in the 7-11.5 GHz frequency range, where intense [a]R-branches are indicated in red. A small portion of the spectrum is highlighted: the red dots indicate the rotational transitions of the monomer, while a few selected transitions of its water cluster are highlighted using blue triangle marks to illustrate the difference in intensity.

conformer 1 to be the global minimum, while MP2 reverses the order. Including the entropic contribution further magnifies this difference.

In the next step, we transitioned to the experimental work. Due to the high melting point of SA (m.p. 165°C), conventional heating evaporation methods resulted in a considerably low proportion of SA in the gas phase. This problem can be overcome by using laser ablation techniques, which have proven successful for many biomolecules.[33–35] Consequently, neutral molecules of sulfanilamide were transferred from its solid into the gas phase using picosecond laser pulses, to measure its rotational spectrum. The spectrum was measured using two different broadband Fourier transform microwave spectrometers (LA-CP-FTMW) that operate in different frequency regions.[21–23] Figure 2 shows a portion of the obtained rotational spectrum, while the whole spectrum can be found in Figure SI01 of the Electronic Supplementary Information (ESI). As can be seen, the spectrum consists of many rotational transitions. Most of the lines showed a not well-resolved hyperfine structure arising due to the presence of two ^{14}N nuclei with non-zero electric quadrupole moment (I=1), which disappeared when the laser was turned off. These two factors indicate that the spectrum must correspond to sulfanilamide species.

Table 1 shows the calculated values for the stable species of the SA monomer. The first thing to realize is that all the conformers have a very high dipole moment on the *a*-axis. The transitions arising from such selection rules usually present a characteristic pattern, so their spectral signatures were first pursued. This strategy lets us obtain a preliminary set of rotational constants for a first rotamer, determined from a rigid rotor analysis.[36] These initial rotational constants helped us quickly locate another series of *c*-type transitions, which were also added to the fit. As a result, 109 transitions were measured (see Table SI01 of the ESI for a complete list of the measured

Table 1 Experimental spectroscopic parameters obtained for the detected rotamers of SA and its water cluster, compared with those calculated using B3LYP-D3(BJ)/6-311++G(d,p) for the lowest energy conformers.

	EXPERIMENTAL	*SA THEORY(B3LYP-D3(BJ)/ MP2)*				*EXPERIMENTAL*	*SA-W THEORY(B3LYP-D3(BJ)*		
Specie	*Rotamer I (LA-MB-FTMW)*	*e-d*	*e-u*	*s-d*	*s-u*	Rotamer II (LA-CP-FTMW)	s-WI	e-WII	e-WIII
A^a	2610.4103(21)[g]	2553/2556	2553/2555	2554/2557	2554/2557	1411.3989(64)	1407	1467	1922
B	565.02163(30)	559/561	559/561	558/560	558/560	504.6184(13)	506	475	410
C	513.47983(26)	508/510	508/510	507/508	507/508	403.6054(13)	404	396	365
$\lvert\mu_a\rvert$	Observed	4.8/4.1	4.8/4.0	7.0/6.4	7.0/6.4	Observed	5.1	3.4	5.1
$\lvert\mu_b\rvert$	Not Observed	0.1/0.1	0.1/0.1	0.0/0.0	0.0/0.0	Observed	2.9	1.9	2.6
$\lvert\mu_c\rvert$	Observed	2.2/1.9	3.8/4.0	2.8/2.4	4.4/4.5	Observed	1.4	0.8	1.0
χ_{aa},*A*	2.4901(56)	2.66/2.54	2.51/2.34	2.68/2.57	2.52/2.34		2.66	2.77	2.41
χ_{bb},*A*	1.8486(75)	2.22/1.94	2.23/1.95	2.21/1.94	2.24/1.95		2.18	1.67	2.24
χ_{cc},*A*	-4.3386(75)	-4.88/-4.48	-4.74/-4.29	-4.89/-4.50	-4.76/-4.29		-4.84	-4.44	-4.65
χ_{aa},*S*	-2.4632(36)	-2.57/-2.45	-2.59/-2.57	-5.01/-4.66	-5.01/-4.70		-3.99	-2.35	-1.83
χ_{bb},*S*	1.3060(64)	0.88/0.88	0.91/1.06	1.79/1.70	1.80/1.71		0.78	1.30	-0.54
χ_{cc},*S*	1.1572(64)	1.69/1.57	1.68/1.51	3.22/2.96	3.22/2.96		3.21	1.05	2.38
ΔE^b	-	0/0	26/28	141/26	202/94		0	154	263
$\Delta E_{ZPE}{}^c$	-	0/4	23/0	229/144	270/226		0	55	128
ΔG^d	-	0/81	37/0	472/427	507/512		283	0	6
N^e	32	-	-	-	-	107			
σ^f	2.5	-	-	-	-	67.5			

[a]*A*, *B*, and *C* are the rotational constants (in MHz); $\lvert\mu_a\rvert$, $\lvert\mu_b\rvert$, and $\lvert\mu_c\rvert$ represent the absolute values of the electric dipole moment components (in D); χ_{aa}, χ_{bb}, and χ_{cc}, are the diagonal elements of the ^{14}N nuclear quadrupole coupling tensor (in MHz); *A* and *S* labels make reference to the amino and sulfonil nitrogen atoms, respectively. [b]Calculated relative energies (in cm^{-1}) to the global minimum. [c]Calculated relative energies (in cm^{-1}) concerning the global minimum, considering the zero-point energy (ZPE). [d]Calculated Gibbs energies (in cm^{-1}) calculated at 298 K. [e]Number of measured transitions. [f]RMS deviation of the fit (in kHz). [g]Standard error in parentheses in units of the last digit.

transitions), allowing us to determine the rotational constants accurately. The obtained rotational constants are *A*=2610.6, *B*=565.0, and *C*=513.5 MHz. We also detected some of the corresponding isotopomers (see Figure SI02 and Tables SI02 to SI05 of the ESI for detailed information): ^{34}S, $^{13}C_2$ (equivalent to $^{13}C_6$), $^{13}C_3$ (equivalent to $^{13}C_5$), and $^{13}C_4$.

Removing the rotational transitions corresponding to the parent SA and its isotopologues resulted in a spectrum with very weak lines. Surprisingly, none of them corresponded to any of the predicted conformers of SA. Therefore, we explored the possibility of them belonging to its hydrated clusters. Following the same strategy as that described above for SA, we first conducted a conformational search of the monohydrated cluster of SA. Among the most stable species, six relevant structures within 150 cm^{-1} respect to the global minimum, shown in Figure 1, were found. All the calculated structures and relevant spectroscopic parameters can be found in Figure SI03 and Table SI06 of the ESI, respectively. Similar to the monomer, the characteristic pattern of the *a*-type progressions was recognizable. In opposition to the monomer, *b*- and *c*-type transitions were also observed in this case. The appearance of the *b*-type transitions was key to confirming the presence of SA-H_2O clusters because, as shown in Table 1, only the monohydrated species presented activity around this axis. A total of 107 rotational transitions were fitted, resulting in the rotational constants collected in Table 1, and corresponding to rotamer II. The complete list of the measured transitions can be found in Table SI07 of the ESI.

For the conformational assignment, we compared the experimental rotational constants and dipole moment components with the calculated values. As expected, the rotational constants of rotamer I are similar to those calculated for SA. However, Table1 shows that the four structures have similar rotational constants. As shown in Figure 1, the four most stable species of SA maintain the same heavy atom skeleton, with the only difference being the position of the NH_2 hydrogens: i.e., the amino group of the sulfonyl amine can be oriented opposite to the aromatic ring (eclipsed, *e*) or towards it (staggered, *s*); additionally, the benzyl NH_2 group can point in the same direction of the sulfonyl amine group (up, *u*) or opposite to it (down, *d*). This slight difference does not cause a significant change in the mass distribution and, consequently, in the rotational constants' values.

Therefore, the rotational constants do not allow an unequivocal conformational identification. However, the diagonal elements of the nuclear quadrupole coupling tensor of each of the ^{14}N can be used for an accurate assignment, as they greatly depend on the chemical environment of each nitrogen atom. The two ^{14}N nuclei of the amine groups of sulfanilamide have a non-zero quadrupole moment (*I*=1), which interacts with the electric field gradient at the site of these nuclei resulting in a hyperfine structure for all the rotational transitions.[37] The nuclear quadrupole coupling constants (χ_{aa}, χ_{bb}, χ_{cc}) extracted from its analysis provide information on the electronic environment of the nitrogen nuclei. In the case of the conformers of sulfanilamide, this information is crucial as it gives the orientations of the two NH_2 groups, allowing us to differentiate between the eclipsed and staggered configurations.

In the next step, we measured selected rotational transitions using our narrow-band Fourier transform microwave spectrometer (LA-MB-FTMW)[24,38,39] to resolve the hyperfine structure completely (see Figures SI04 and SI05 of the ESI). A total of 32 components were measured, obtaining the spectroscopic values listed in Table 1 for rotamer I (see Table SI08 of the ESI for a complete list of the measured transitions). The nuclear quadrupole coupling constants around the sulfanyl nitrogen atom indicate that rotamer I must correspond to an *eclipsed* configuration, which is also the most stable configuration. It settles down the *staggered* vs. *eclipsed* problem. However, the *up* and *down* configurations show similar rotational and quadrupole coupling constants and cannot be distinguished solely.

To discern between both orientations, we explored the dependence of the intensity on the polarization power in a linear regime. As shown in Table 1, the *eclipsed-up* configuration has an almost similar dipole moment for the *a*- and *c*-type components (1:1 ratio), while the *eclipsed-down* configuration has twice the dipole moment value for the *a*-type component with respect to the *c*-type (2:1 ratio). Therefore, we compared the effect of the polarization power change on *a*- and *c*-type transitions using the MB-FTMW technique, as it ensures a linear regime. The results are shown in Figures SI04 and SI05: while a severe attenuation of the polarization power only shows the *a*-type transitions, increasing the polarization power results in an increase of the *a*-type transitions and the appearance of the *c*-type transitions. Further increasing the polarization power saturates the *a*-type transitions and increases *c*-type transitions until saturation is reached. This dependence is expected for a situation where $\mu_a > \mu_c$, is in good agreement with the *eclipsed-down* configuration. We estimate twice the dipole moment for the *a*-type transitions with respect to the *c*-type transitions, in excellent agreement with the predicted value of such configuration. Therefore, the experiments point to the *eclipsed-down* configuration as the experimentally detected conformer. Nevertheless, it also exists the possibility of a vibrationally averaged system.[17]

According to their energetics, there are four conformers of sulfanilamide which should be stable enough to be present in the experiment, but a single structure has been observed. The other three predicted structures must be missing due to the properties of the supersonic expansion.[40–43] We performed a relaxed Potential Energy Surface (PES) scan to estimate the interconversion barrier energy. The results are collected in Figure SI06 of the ESI and show that the inversion of the benzylic amine that connects the *up* and *down* configurations are separated by an energetic barrier of less than 100 cm^{-1}, confirming a conformational interconversion. Additionally, the *eclipsed* and *staggered* conformations are connected by an S-NH_2 inversion. We located the transition state and estimated an interconversion barrier of ~500 cm^{-1} (see Figure SI06 of the ESI). This value is within the limit for conformational interconversion. Therefore, a partial interconversion together with its lower stability explains its non-detection. Nevertheless, the four

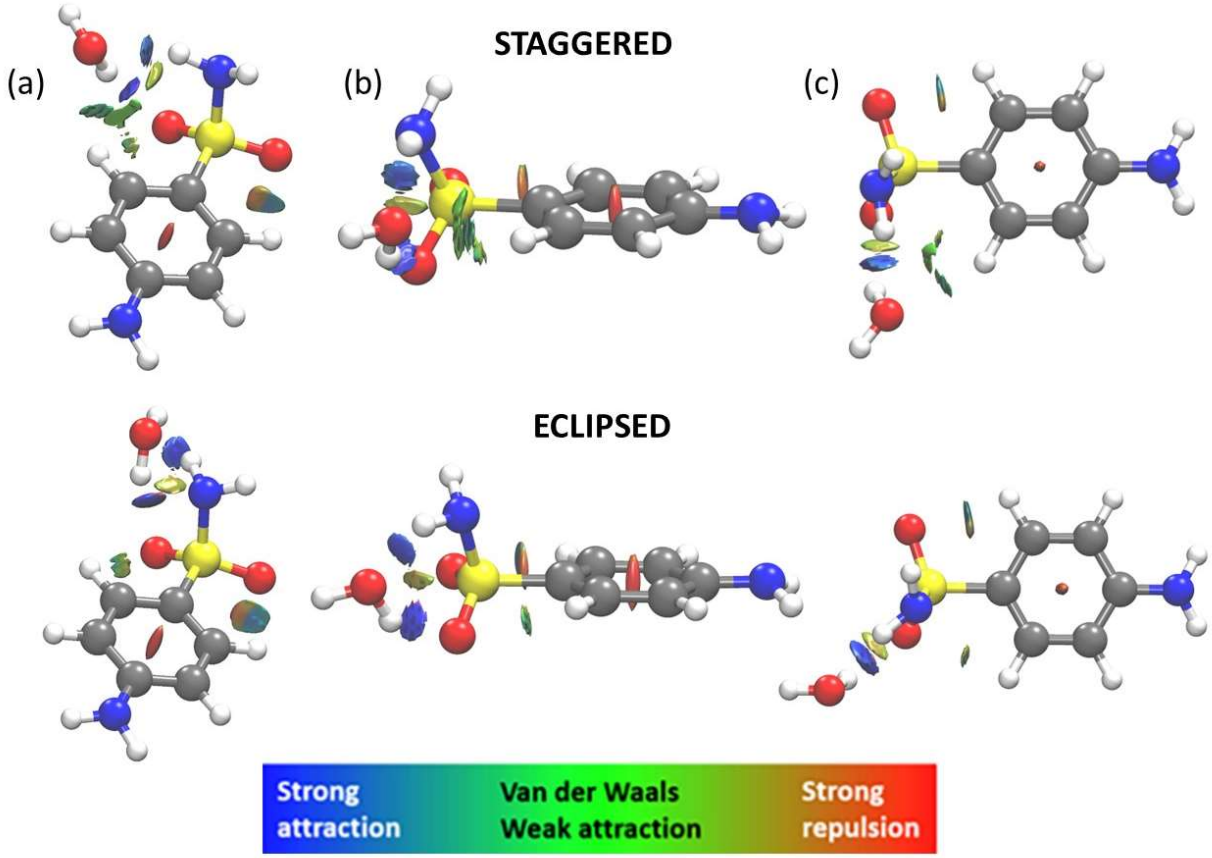

Figure 3 Comparison between the NCIplots of the eclipsed (top) and staggered (bottom) configurations of the SA-H_2O cluster using different views for an easier visualization: (a) Isometric, (b) side and (c) top views. Red surfaces correspond to strong repulsion forces, blue surfaces to strong attraction forces and green surfaces to weak attractive interactions.. An isovalue os 0.35 was used.

conformers should be interconverting from one to another at the room temperature of the physiological conditions.

Once the conformational puzzle of SA is solved, we focus on analyzing its water cluster. There are several structures for the SA-H_2O cluster, but all of them are based on the bare molecule: the water molecule enters interacting with either the *eclipsed* or the *staggered* configurations of SA. There are also some minor variations in the relative position of water within each configuration, but they are separated by shallow interconversion barriers and, therefore, only the three structures collected in Table 1 are relevant. The nuclear quadrupole coupling interactions of the two ^{14}N nuclei of sulfanilamide-water result in a very complex hyperfine structure for all observed rotational lines. No attempt was made to assign the quadrupole hyperfine components due to the weakness of transitions, and no information about the quadrupole coupling constants was obtained. The rotational frequencies were measured as the intensity-weighted mean of the line cluster, which could affect the uncertainty of frequency measurements reflected in a larger RMS value (see Table 1). However, the rotational constants alone can distinguish between both configurations. The excellent matching between the experimental and calculated rotational constants shows that water prefers to interact with the SA in the *staggered* configuration. This unambiguos determination of the *staggered* configuration is in good agreement with the results reported by Müller et at.[17] The absence of the eclipsed configuration can be explained by conformational interconversion, as in the bare molecule. In this case, the barrier separating both structures is calculated to be ~350 cm^{-1} (see Figure SI07 of the ESI), explaining the presence of a single conformer in the supersonic expansion.

Once the structural identification has been made, we can extract some information about the intramolecular interactions in the molecule. The case of sulfanilamide is exciting: The *staggered* configuration has an additional stabilization due to the N-H•••π interaction, while the *eclipsed* configuration loses such interaction in favour of two N-H•••O=S interactions. Calculations using DFT methods at B3LYP-D3(BJ) estimate that the conformer with the N-H•••π interaction is 230 cm^{-1} less stable, while MP2 methods yield a similar value (144 cm^{-1}). The experimental results confirm that the N-H•••O=S interaction gives more stability to the molecule.

Regarding the SA-H_2O cluster, the most stable structures are those where water acts as a proton donor to the sulfanilamide molecule via an O-H•••O=S hydrogen bond and, on the other

hand, it acts as a proton acceptor with the sulfanilamide's amino group via an N-H•••O hydrogen bond. This arrangement allows the cluster to form a cyclic hydrogen network and confers the molecule, both for the *eclipsed* or *staggered* configuration, a great stability. Interestingly, the experimental results show that the *staggered* configuration is more stable, in opposition to the bare molecule where the *eclipsed* form is preferred. In order to explain such stabilization, we evaluated the intramolecular interactions of the eclipsed and staggered configurations of SA-H_2O using an NCIplot analysis.[44,45] The comparison is shown in Figure 3, and confirms the stabilization of both configurations through a strong N-H•••O-H•••O=S hydrogen bond network. The plot also shows that the *staggered* configuration has an additional C-H•••O intermolecular interaction, stabilizing its structure over the *eclipsed* configuration. We also quantified the preference of the *staggered* configuration by calculating the dissociation energies (D_0) of both configurations using B3LYP-D3(BJ)/6-311++G(d,p): the *staggered* form has a dissociation energy of 39.0 kJ mol^{-1}, while that of the *eclipsed* conformation is 33.6 kJ mol^{-1}. This value is considerably high (see Table SI09 of the ESI for a comparison with other systems) and shows that the cluster is very stable. The results above are exciting as there is a conformational switch: the *eclipsed* configuration in the bare molecule switches to the *staggered* configuration when water is introduced. Therefore, a single water molecule acts as a conformational selector.

Conclusions

We have characterized the conformational preferences of the sulfanilamide monomer and its monohydrated cluster in the isolated conditions of the gas phase using laser ablation techniques combined with rotational spectroscopy. Chirped pulse Fourier-transform microwave (LA-CP-FTMW) spectroscopy allowed the detection of the most abundant species for each species. Additionally, for the monomer the nuclear quadrupole coupling constants have been obtained using molecular-beam Fourier-transform microwave (LA-MB-FTMW) spectroscopy.

We have identified unequivocally one conformer for both, sulfanilamide and its water cluster, and evaluated the intra- and inter-molecular interactions that govern the structures. We show that a single water molecule can modify the conformational preferences of the monomer.

Conflicts of interest

There are no conflicts to declare.

Acknowledgements

The financial funding from Ministerio de Ciencia e Innovación (PID2019-111396GB-I00), Junta de Castilla y León (VA244P20) and European Research Council under the European Union's Seventh Framework Programme (FP/2007-2013) / ERC-2013-SyG, Grant Agreement n. 610256 NANOCOSMOS, are gratefully acknowledged. S.M. thanks Consejo Social from Universidad de Valladolid for an undergraduate fellowship.

Notes and references

1 P. Gelmo, cber Sulfamide der p-bmidobenzolsalfonsaure;, *J. für Prakt. Chemie*, 1908, **77**, 369–382.

2 G. Domagk, Ein Beitrag zur Chemotherapie der bakteriellen Infektionen, *Dtsch. Medizinische Wochenschrift*, 1935, **61**, 250–253.

3 D. D. Woods, The Biochemical Mode of Action of the Sulphonamide Drugs, *J. Gen. Microbiol.*, 1962, **29**, 687–702.

4 A. Achari, D. O. Somers, J. N. Champness, P. K. Bryant, J. Rosemond and D. K. Stammers, Crystal structure of the anti-bacterial sulfonamide drug target dihydropteroate synthase, *Nat. Struct. Biol.*, 1997, **4**, 490–497.

5 O. Sköld, Sulfonamide resistance: mechanisms and trends, *Drug Resist. Updat.*, 2000, **3**, 155–160.

6 F. F. Nord and C. M. Werkman, *Advances in enzymology and related areas of molecular biology*, wiley, 2006, vol. 4.

7 B. H. O'Connor and E. N. Maslen, The crystal structure of α-sulphanilamide, *Acta Crystallogr.*, 1965, **18**, 363–366.

8 M. ALLEAUME and J. DECAP, Affinement Tridimensionnel Du Sulfanilamide Beta., *Acta Crystallogr.*, 1965, **18**, 731–736.

9 M. Alléaume and J. Decap, Affinement tridimensionnel du sulfanilamide gamma., *Acta Crystallogr.*, 1965, **19**, 934–938.

10 A. M. O'Connell and E. N. Maslen, X-ray and neutron diffraction studies of beta-sulphanilamide., *Acta Crystallogr.*, 1967, **22**, 134–145.

11 T. Gelbrich, A. L. Bingham, T. L. Threlfall and M. B. Hursthouse, -Sulfanilamide, *Acta Crystallogr. Sect. C Cryst. Struct. Commun.*, 2008, **64**, 205–207.

12 A. Portieri, R. K. Harris, R. A. Fletton, R. W. Lancaster and T. L. Threlfall, Effects of polymorphic differences for sulfanilamide, as seen through 13C and 15N solid-state NMR, together with shielding calculations, *Magn. Reson. Chem.*, 2004, **42**, 313–320.

13 L. Frydman, A. C. Olivieri, L. E. Diaz, B. Frydman, A. Schmidt and S. Vega, A13C solid-state NMR study of the structure and the dynamics of the polymorphs of sulphanilamide, *Mol. Phys.*, 1990, **70**, 563–579.

14 A. D. Popova, M. K. Georgieva, O. I. Petrov, K. V. Petrova and E. A. Velcheva, IR spectral and structural studies of 4-aminobenzenesulfonamide (sulfanilamide)-d0, -d4, and -15N, as well as their azanions: Combined DFT B3LYP/experimental approach, *Int. J. Quantum Chem.*, 2007, **107**, 1752–1764.

15 G. Ogruc Ildiz and S. Akyuz, Conformational analysis and vibrational study of sulfanilamide, *Vib. Spectrosc.*, 2012, **58**, 12–18.

16 A. Borba, A. Gómez-Zavaglia and R. Fausto, Conformational landscape, photochemistry, and infrared spectra of sulfanilamide, *J. Phys. Chem. A*, 2013, **117**, 704–717.

17 T. Uhlemann, S. Seidel and C. W. Müller, Laser desorption single-conformation UV and IR spectroscopy of the sulfonamide drug sulfanilamide, the sulfanilamide-water complex, and the sulfanilamide dimer, *Phys. Chem. Chem. Phys.*, 2017, **19**, 14625–14640.

18 I. N. Kolesnikova, A. N. Rykov, V. V Kuznetsov and I. F. Shishkov, Joint gas-phase electron diffraction and quantum chemical study of conformational landscape and molecular structure of sulfonamide drug sulfanilamide, *Struct. Chem.*, 2020, **31**, 1353–1362.

19 A. Vigorito, C. Calabrese, A. Maris, D. Loru, I. Peña, M. E. Sanz and S. Melandri, The Shapes of Sulfonamides: A Rotational Spectroscopy Study, *Molecules*, 2022, **27**, 2820.

20 I. León, E. R. Alonso, S. Mata and J. L. Alonso, Shape of Testosterone, *J. Phys. Chem. Lett.*, 2021, **12**, 6983–6987.

21 G. G. Brown, B. C. Dian, K. O. Douglass, S. M. Geyer, S. T. Shipman and B. H. Pate, A broadband Fourier transform microwave spectrometer based on chirped pulse excitation, *Rev. Sci. Instrum.*, 2008, **79**, 053103.

22 S. Mata, I. Pena, C. Cabezas, J. C. López and J. L. Alonso, A broadband Fourier-transform microwave spectrometer with laser ablation source: The rotational spectrum of nicotinic acid, *J. Mol. Spectrosc.*, 2012, **280**, 91–96.

23 I. Peña, S. Mata, A. Martín, C. Cabezas, A. M. Daly and J. L. Alonso, Conformations of D-xylose: the pivotal role of the intramolecular hydrogen-bonding., *Phys. Chem. Chem. Phys.*, 2013, **15**, 18243–8.

24 J. Grabow, W. Stahl and H. Dreizler, A multioctave coaxially oriented beam-resonator arrangement Fourier-transform microwave spectrometer, *Rev. Sci. Instrum.*, 1998, **67**, 4072.

25 I. León, E. R. Alonso, S. Mata, C. Cabezas, M. A. Rodríguez, J.-U. Grabow and J. L. Alonso, The role of amino acid side chains in stabilizing dipeptides: the laser ablation Fourier transform microwave spectrum of Ac-Val-NH 2, *Phys. Chem. Chem. Phys.*, 2017, **19**, 24985–24990.

26 2018. Schrödinger Release 2018-3: Maestro Schrödinger, LLC, New York, NY, .

27 C. Møller and M. S. Plesset, Note on an approximation treatment for many-electron systems, *Phys. Rev.*, 1934, **46**, 618–622.

28 A. D. Becke, Density-functional exchange-energy approximation with correct asymptotic behavior, *Phys. Rev. A*, 1988, **38**, 3098–3100.

29 A. D. Becke, A new mixing of Hartree-Fock and local density-functional theories, *J. Chem. Phys.*, 1993, **98**, 1372–1377.

30 Y. Zhao and D. G. Truhlar, Density functionals for noncovalent interaction energies of biological importance, *J. Chem. Theory Comput.*, 2007, **3**, 289–300.

31 M. J. Frisch, J. A. Pople and J. S. Binkley, Self-consistent molecular orbital methods 25. Supplementary functions for Gaussian basis sets, *J. Chem. Phys.*, 1984, **80**, 3265–3269.

32 S. Grimme, J. Antony, S. Ehrlich and H. Krieg, A consistent and accurate ab initio parametrization of density functional dispersion correction (DFT-D) for the 94 elements H-Pu, *J. Chem. Phys.*, 2010, **132**, 154104.

33 I. Peña, C. Cabezas and J. L. Alonso, The nucleoside uridine isolated in the gas phase, *Angew. Chemie - Int. Ed.*, 2015, **54**, 2991–2994.

34 J. L. Alonso and J. C. López, in *Gas-Phase IR Spectroscopy and Structure of Biological Molecules*, eds. A. M. Rijs and J. Oomens, Topics in., 2015, vol. 364, pp. 335–402.

35 E. R. Alonso, I. León and J. L. Alonso, in *Intra- and Intermolecular Interactions Between Non-covalently Bonded Species*, Elsevier, 2021, pp. 93–141.

36 H. M. Pickett, The fitting and prediction of vibration-rotation spectra with spin interactions, *J. Mol. Spectrosc.*, 1991, **148**, 371–377.

37 W. Gordy, *Microwave molecular spectra*, Wiley-Interscience, New York, 3rd ed., 1984.

38 I. León, E. R. Alonso, C. Cabezas, S. Mata and J. L. Alonso, Unveiling the n→π* interactions in dipeptides, *Commun. Chem.*, 2019, **2:3**, 1-8.

39 J. L. Alonso, V. Vaquero, I. Peña, J. C. López, S. Mata and W. Caminati, All five forms of cytosine revealed in the gas phase, *Angew. Chemie - Int. Ed.*, 2013, **52**, 2331–2334.

40 R. S. Ruoff, T. D. Klots, T. Emilsson and H. S. Gutowsky, Relaxation of conformers and isomers in seeded supersonic jets of inert gases, *J. Chem. Phys.*, 1990, **93**, 3142–3150.

41 P. D. Godfrey, R. D. Brown and F. M. Rodgers, The missing conformers of glycine and alanine: relaxation in seeded supersonic jets, *J. Mol. Struct.*, 1996, **376**, 65–81.

42 I. León, E. R. Alonso, S. Mata and J. L. Alonso, A rotational study of the AlaAla dipeptide, *Phys. Chem. Chem. Phys.*, 2020, **22**, 13867–13871.

43 C. Cabezas, M. Varela and J. L. Alonso, The Structure of the Elusive Simplest Dipeptide Gly-Gly, *Angew. Chemie Int. Ed.*, 2017, **129**, 6520–6525.

44 E. R. Johnson, S. Keinan, P. Mori-Sánchez, J. Contreras-García, A. J. Cohen and W. Yang, Revealing noncovalent interactions, *J. Am. Chem. Soc.*, 2010, **132**, 6498–6506.

45 J. Contreras-García, E. R. Johnson, S. Keinan, R. Chaudret, J. P. Piquemal, D. N. Beratan and W. Yang, NCIPLOT: A program for plotting noncovalent interaction regions, *J. Chem. Theory Comput.*, 2011, **7**, 625–632.